THE JOURNAL OF BIOLOGICAL CHEMISTRY Vol. 276, No. 28, Issue of July 13, pp. 26148–26153, 2001
Printed in U.S.A.

Mechanism of Rhodopsin Activation as Examined with Ring-constrained Retinal Analogs and the Crystal Structure of the Ground State Protein*

Received for publication, March 12, 2001, and in revised form, April 18, 2001
Published, JBC Papers in Press, April 20, 2001, DOI 10.1074/jbc.M102212200

Geeng-Fu Jang‡§, Vladimir Kuksa‡§, Stawomir Filipek¶, Franz Bartl‖, Eglof Ritter‖, Michael H. Gelb‡‡, Klaus Peter Hofmann‖, and Krzysztof Palczewski‡**§§¶¶**

*From the Departments of ‡Ophthalmology, §§Pharmacology, **Chemistry, and ‡‡Biochemistry, University of Washington, Seattle, Washington 98195, the ¶Department of Chemistry, University of Warsaw, 1 Pasteur Street, Warsaw PL-02093 Poland, and the ‖Institut für Medizinische Physik und Biophysik, Universitätsklinikum Charité, Humboldt Universität zu Berlin, Berlin D-10098, Germany*

The guanine nucleotide-binding protein (G-protein)-coupled receptor superfamily (GPCR) is comprised of a large group of membrane proteins involved in a wide range of physiological signaling processes. The functional switch from a quiescent to an active conformation is at the heart of GPCR action. The GPCR rhodopsin has been studied extensively because of its key role in scotopic vision. The ground state chromophore, 11-*cis*-retinal, holds the transmembrane region of the protein in the inactive conformation. Light induces *cis-trans* isomerization and rhodopsin activation. Here we show that rhodopsin regenerated with a ring-constrained 11-*cis*-retinal analog undergoes photoisomerization; however, it remains marginally active because isomerization occurs without the chromophore-induced conformational change of the opsin moiety. Modeling the locked chromophore analogs in the active site of rhodopsin suggests that the β-ionone ring rotates but is largely confined within the binding site of the natural 11-*cis*-retinal chromophore. This constraint is a result of the geometry of the stable 11-*cis*-locked configuration of the chromophore analogs. These results suggest that the native chromophore *cis-trans* isomerization is merely a mechanism for repositioning of the β-ionone ring which ultimately leads to helix movements and determines receptor activation.

Binding of specific ligands to the extracellular or conserved seven α-helical transmembrane domains of guanine nucleotide-binding protein (G-protein)[1]-coupled receptors (GPCRs) causes conformational changes that act as a switch to relay the signal to heterotrimeric G-proteins, which in turn evoke subsequent intracellular responses. Understanding the precise conformational transformation of an inactive GPCR into an activated form capable of interacting with a G-protein is a key problem in elucidating the molecular steps of cell surface receptor signaling. Rhodopsin, a member of the GPCR family, is involved in photon absorption in retinal rod cells and activation of transducin, a specific G-protein (1). Rhodopsin is a bipartite molecule composed of the protein opsin (~40 kDa) and 11-*cis*-retinal (a derivative of vitamin A), which is covalently linked to opsin through a protonated Schiff base with Lys^{296} located in transmembrane helix VII (H-VII) (1–3). The determination of the x-ray structure of the first GPCR, rhodopsin, provides new insights into the ground state conformation of this receptor (5). The inactive conformation of rhodopsin is stabilized by the 11-*cis*-retinal chromophore. The positive charge of the Schiff base linkage is placed in a highly hydrophobic environment and is neutralized by Glu^{113} (6, 7). Absorption of a photon by the chromophore causes photoisomerization around the $C_{11}=C_{12}$ double bond and the formation of all-*trans*-retinylidene (8). Photoisomerization of the chromophore to the all-*trans* isomer causes changes in the polyene chain of the chromophore, including reorientation of the C_9 and C_{13} methyl groups and repositioning of the β-ionone ring, which ultimately leads to deprotonation of the Schiff base and changes at the cytoplasmic surface of rhodopsin (3). These changes are sufficient to drive a conformational change of the protein and transient activation of opsin before the Schiff base hydrolyzes to release all-*trans*-retinal from opsin. The atomic resolution structures of these intermediates are not yet available.

The activation process of rhodopsin has been investigated by biochemical methods, and several models have been proposed. In one of the most widely accepted models, it is proposed that photoactivation involves a critical proton transfer between the protonated Schiff base and the glutamate counter-ion. However, it is clear that the structural constraint imposed on opsin by the protonated Schiff base–counter-ion interaction can account only partially for the receptor inactivation (4). The photoactivation process could also involve the repositioning of the methyl groups of all-*trans*-retinal compared to 11-*cis*-retinal, particularly movement of the methyl group at C_9 could cause activation by triggering a conformational change in opsin (2). Retinal analogs, with a bridge between C_{10} and C_{13} of 1–4 carbons which prevents isomerization around the $C_{11}=C_{12}$ bond, stabilize opsin in its inactive conformation (or minimally active) even under light conditions (9–11). It is believed that lack of isomerization or incomplete isomerization around the $C_{11}=C_{12}$ bond in the polyene chain of the retinal analog is the

* This work was supported by National Institutes of Health Grant EY09339 (to K. P.), a grant from Research to Prevent Blindness, Inc. to the Department of Ophthalmology at the University of Washington, and grants from the Foundation Fighting Blindness, Inc., the Ruth and Milton Steinbach Fund, and the E. K. Bishop Foundation. The costs of publication of this article were defrayed in part by the payment of page charges. This article must therefore be hereby marked "*advertisement*" in accordance with 18 U.S.C. Section 1734 solely to indicate this fact.

§ These authors contributed equally to this work.

¶¶ Senior Scientific Investigator of Research to Prevent Blindness, Inc. To whom correspondence should be addressed: Dept. of Ophthalmology, University of Washington, Box 356485, Seattle, WA 98195-6485. Tel.: 206-543-9074; Fax: 206-221-6784; E-mail: palczews@u.washington.edu.

[1] The abbreviations used are: G-protein, guanine nucleotide-binding protein; GPCR, G-protein-coupled receptor; HPLC, high performance liquid chromatography; BTP, 1,3-bis(tris(hydroxymethyl)-methylamino)propane; FTIR, Fourier transform infrared spectroscopy; RDH, retinol dehydrogenase; MES, 4-morpholineethanesulfonic acid.

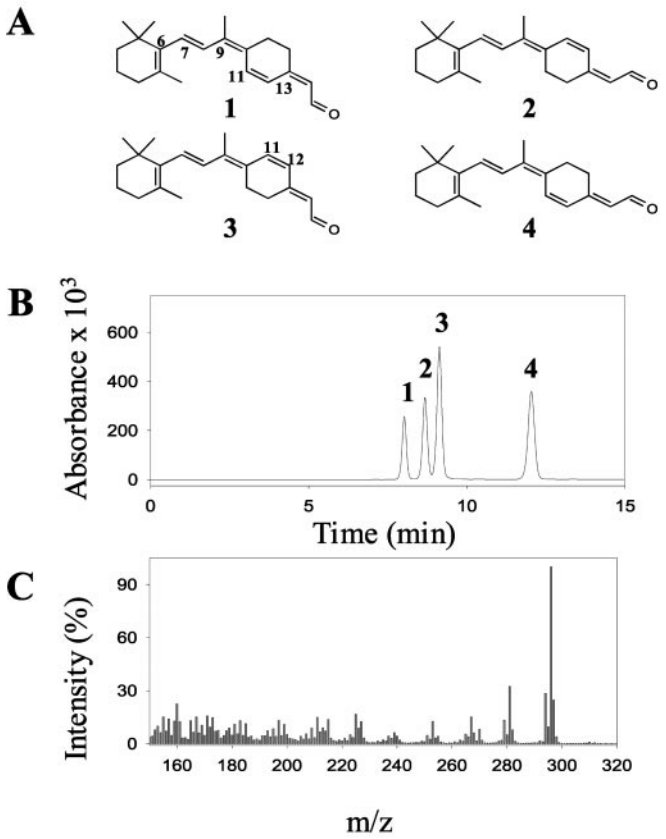

FIG. 1. *Panel A*, structures of the four 11-*cis*-locked retinal analog isomers. *Panel B*, chromatographic separation of the isomeric mixture of 11-*cis*-locked retinal analogs using 4% ethyl acetate in hexane, and normal phase HPLC on a silica column. *Panel C*, electron impact mass spectrum (37) of the 11-*cis*-locked isomer mixture, showing the corresponding molecular ion peak at 296 *m/z*. The conformation about the C_6–C_7 single bond for analogs **1–4** is shown in the 6-s-*cis* configuration.

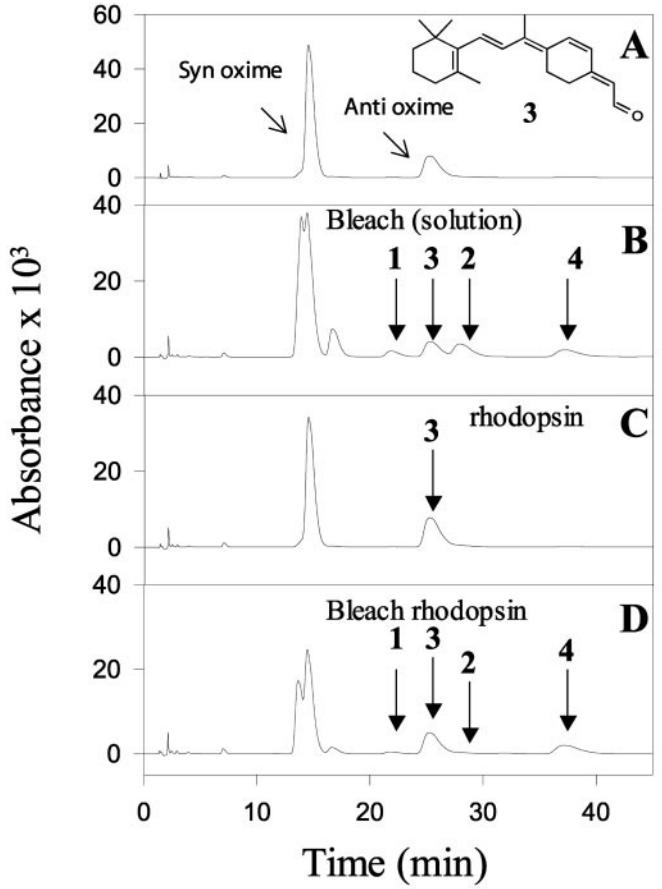

FIG. 2. **Normal phase HPLC analysis of the *syn*- and *anti*-oxime derivatives of 11-*cis*-locked retinal isomer 3 in solution (*panels A* and *B*) and in rhodopsin (*panels C* and *D*) without (*panels A* and *C*) or with photobleaching (*panels B* and *D*).** The rhodopsin reconstituted from opsin and 11-*cis*-locked retinal isomer **3** was solubilized with *n*-dodecyl-β-D-maltoside and purified using a concanavalin A-Sepharose 4B column (38). The purified fraction was subjected to photobleaching, and the chromophore(s) was derivatized with hydroxylamine and analyzed by HPLC (see "Experimental Procedures") (13, 36). As a control, isomer **3** was photobleached in the same elution buffer and analyzed as above. *Arrows* show the elution positions of the *anti*-oximes derived from isomers **1–4**.

cause of this lack of rhodopsin activation. Alternatively, the repositioning of the β-ionone ring of the chromophore may be needed to trigger conformational changes that lead to the formation of the active form of rhodopsin. We revisited this problem using ring-constrained ("locked") retinal analog regenerated rhodopsins and the three-dimensional structure of rhodopsin in the ground state to understand what changes within the chromophore binding pocket are allowed without substantial receptor activation.

EXPERIMENTAL PROCEDURES

Synthesis—Two isomeric cyclic ketones (9-*cis*- and 9-*trans*-) containing four double bonds were prepared by condensation between β-ionone and 3-methoxy-2-cyclohexenone followed by subsequent reduction, hydrolysis and water elimination (12). Horner-Emmons reaction of the ketone followed by diisobutylaluminium hydride reduction afforded an isomeric mixture of four 11-*cis*-locked retinal analogs in an approximately equal ratio. The mixture was separated using isocratic normal phase HPLC with 4% ethyl acetate and hexane. Each fraction was rechromatographed additionally using the same conditions to achieve the final isomeric purity of 95–98%.

Photoisomerization of 11-cis-Locked Retinal Analogs of Rhodopsin—Rod outer segments membranes from 50 retinas (~40 mg of rhodopsin) were suspended in 20 ml of H_2O. The suspension was centrifuged at 110,000 × *g* for 30 min. The pellet was resuspended in 20 ml of 20 mM BTP, pH 7.4, 0.1 M NaCl, and 16 mM NH_2OH (freshly prepared), and the mixture was placed on ice and bleached with a 250-watt lamp at a distance of 10 cm for 30 min. The bleached rhodopsin (opsin) was washed extensively with 20 mM BTP, pH 7.4, 0.1 M NaCl and finally suspended in 10 ml of the same buffer. The above opsin suspension (350 μl) was mixed with ~54 nmol of 11-*cis*-locked retinal analog in *N*,*N*-dimethylformamide or *N*,*N*-dimethylformamide only (9 μl) as a control, and the mixture was incubated on a nutator at room temperature overnight under dim red light conditions. The reconstituted rhodopsin analog was then solubilized with 10 mM *n*-dodecyl-β-D-maltoside, and the solubilization mixture was centrifuged at 86,000 × *g* for 15 min. The resulting supernatant was loaded onto 0.7 ml of concanavalin A-Sepharose 4B (Sigma) equilibrated with buffer A (20 mM BTP, pH 7.4, 10 mM *n*-dodecyl β-D-maltoside, 0.1 M NaCl) in a glasswool plug Pasteur pipette at 10 °C. The column was washed with 15 column volumes of buffer A (monitored by the disappearance of UV absorption at ~350 nm), and the fractions containing rhodopsin analogs were eluted with 700 μl of 300 mM methyl α-D-mannopyranoside in buffer A. The purified rhodopsin analogs were bleached twice by a photographic flashlight from a 5-cm distance. The retinoids were converted to their oximes by adding 300 μl of MeOH and 150 μl of 0.4 M NH_2OH, pH 6.5, and the oximes were extracted twice with 500 μl of hexane. Retinoids were analyzed by normal phase HPLC (Alltech, silica 5 μ, 2.1 × 250 mm) with 4% ethyl acetate in hexane at a flow rate of 0.5 ml/min (13).

Purification of Transducin and the Activity Assay—Transducin was purified from bovine ROS as described previously (14). The activity of transducin was determined by following the light-dependent binding of [^{35}S]GTPγS (2 Ci/mmol) at 28 °C (15). The transducin concentration was 1.5 μM, [^{35}S]GTPγS was 4 μM, and rhodopsin regenerated with 11-*cis*-retinal or **1–4** analogs in native membranes was 5 nM.

FTIR Spectroscopy—To prepare the FTIR samples, 24 μM opsin membranes (16) were incubated overnight with 240 μM native 11-*cis*-retinal or with the mixture of locked retinal analogs in BTP buffer (130 mM NaCl, 20 mM BTP, pH 7.5, 1 mM $MgCl_2$). Suspensions of membranes were centrifuged for 25 min at 100,000 × *g*, yielding 2.2 mM rhodopsin in the pellet (from absorption at 500 nm). The buffer solution was

Retinal	Structure	Isomer	Non-bleached sample in solution				Bleached sample in solution				Non-bleached sample in rhodopsin				Bleached sample in rhodopsin				RDH	
			1	2	3	4	1	2	3	4	1	2	3	4	1	2	3	4	all-*trans*	11-*cis*
1	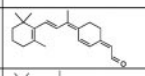	9,11,13-tri-*cis*	94	4	0	2	22	15	22	41	69	0	5	26	34	10	24	32	0	100
2	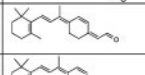	11,13-di-*cis*	0	100	0	0	11	32	34	23	0	18	79	3	9	9	44	38	100	0
3	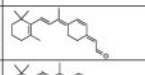	11-*cis*	0	0	100	0	11	33	34	22	0	0	98	2	5	3	58	34	0	100
4	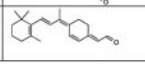	9,11-di-*cis*	0	0	0	100	18	22	23	36	51	1	5	43	37	10	17	36	100	0

FIG. 3. **Oximes produced from each 11-*cis*-locked retinal isomer in solution and in rhodopsin with or without photobleaching and substrate specificities of 11-*cis*- and all-*trans*-RDH toward each isomer.** Oximes were formed in a reaction with hydroxylamine and separated by HPLC (13, 36). The percentages of each isomer (**1**-**4**) are shown. Activities of 11-*cis*-RDH (detergent-purified human recombinant 11-*cis*-RDH or RDHs in retinal pigment epithelium microsomes) and all-*trans*-RDH (recombinant photoreceptor called prRDH or all-*trans*-RDH in rod outer segments) were determined by monitoring the production of the corresponding [15-^{3}H]retinol analog from the reduction of the 11-*cis*-locked retinal analog and pro-*S*-[4-^{3}H]NADH (for 11-*cis*-RDH) or pro-*S*-[4-^{3}H]NADPH (for all-*trans*-RDH) (13). The product was analyzed by normal phase HPLC and quantified by scintillation counting. For example, 11-*cis*-RDH activities with analogs **1** and **3** and pro-*S*-[4-^{3}H]NADH as substrates were 92.3 and 40.1 nmol/min/mg, respectively, but no activity with analogs **2** and **4** could be detected. In contrast, recombinant prRDH activities with analogs **2** and **4** and pro-*S*-[4-^{3}H]NADPH as substrates were 1.33 and 2.33 nmol/min/mg, respectively. No activity was observed with analogs **1** and **3**.

TABLE I
*Rate of transducin activation by rhodopsin and rhodopsin regenerated with **1–4** analogs*

The assay was carried out for 3 min as described under "Experimental Procedures." Rhodopsin was regenerated with 11-cis-retinal or one of the four retinal analogs (**1–4**) (see Fig. 1). The binding was initiated by addition of [^{35}S]GTPγS in the dark or freshly bleached samples. The assay was performed in triplicate.

Sample	Dark activity	Light activity
	pmol bound [^{35}S]GTPγS/min	
Opsin	0.2 ± 0.1	0.2 ± 0.15
Rhodopsin	0.6 ± 0.3	3.6 ± 0.9
Rhodopsin (**1**)	0.4 ± 0.3	0.6 ± 0.3
Rhodopsin (**2**)	0.4 ± 0.3	0.8 ± 0.2
Rhodopsin (**3**)	0.5 ± 0.2	0.8 ± 0.4
Rhodopsin (**4**)	0.6 ± 0.1	0.6 ± 0.3

removed and the pellet transferred to a 30-mm diameter temperature-controlled transmission cell with two BaF_2 windows and a 5-μm teflon gasket. The spectra were recorded using a Bruker ifs 66v spectrometer (17). Measurements were performed at pH 7.5 and 25 °C. For both samples, Meta II minus rhodopsin difference spectra were generated.

HPLC Assay for RDH Activities with 11-cis-Locked Retinal Analogs—Activities of 11-*cis*-retinol dehydrogenase (11-*cis*-RDH) in retinal pigment (prRDH) epithelium microsomes or all-*trans*-retinol dehydrogenase (all-*trans*-RDH) in rod outer segments were assayed by monitoring the production of [15-^{3}H]retinol analogs (reduction of retinal analogs). The reaction mixture (100 μl) contained MES (final concentration, 80 mM, pH 5.5), pro-*S*-[4-^{3}H]NADH (13) (24 μM) for 11-*cis*-RDH (0.31 μg) or RDHs in retinal pigment epithelium (7.5 μg) or pro-*S*-[4-^{3}H]NADPH (27 μM) for prRDH (20.8 μg) or all-*trans*-RDH in rod outer segments (7.5 μg), and 1 μl of 11-*cis*-locked retinal analog (60 μM) substrate added last to initiate the reaction. The reaction was incubated at 33 °C for 10 min, then quenched with 400 μl of MeOH and 100 μl of 1 M NaCl, and extracted with 500 μl of hexane. After mixing and separating phases, 400 μl of the upper phase was removed and dried with a stream of argon. The residue was dissolved in 120 μl of hexane, and 100 μl was analyzed by normal phase HPLC (Beckman, Ultrasphere-Si, 4.6 × 250 mm) with 10% ethyl acetate in hexane for analogs **1** and **4** or 4% ethyl acetate in hexane for analogs **2** and **3** at a flow rate of 1.4 ml/min using an HP1100 with a diode array detector and HP Chemstation A.06.03 software. The corresponding retinol analog fraction was collected and subjected to scintillation counting.

Modeling—Coordinations for bovine rhodopsin were taken from the Protein Data Bank (1F88). Addition of hydrogen atoms and all optimizations were done in Insight II (Insight II release 98.0 (1998), Molecular Simulations Inc., San Diego). The protonation state of amino acid side chains was obtained using standard pK_a values and a pH of 7.0. For molecular dynamics runs with FDiscover (Discover version 2.98, Molecular Simulations Inc.), force field cff91 (18, 19) together with charges of Gasteiger-Marsili (20) were used. All optimization results were confirmed by using CDiscover with esff force field and new charge calculation method. The ESFF force field is a rule-based force field that was developed at Molecular Simulations Inc. The charges are determined by minimizing the electrostatic energy with respect to the charges under the constraint that the sum of the charges is equal to the net charge on the molecule. Retinal and its four locked analogs together with Lys^{296} were optimized with the rest of the protein fixed. The same procedure was applied to residues near (4.5 Å) the movable part of rhodopsin structure. Then the complete protein structure was optimized without constraints. Visualizations were done on a portion of rhodopsin confined to a 4.5 Å radial distance from the retinal and Lys^{296} atoms. It was necessary to remove some of the residues to show the retinal inside the cavity. Additional information is provided in the figure legends.

RESULTS AND DISCUSSION

To obtain additional insight into the activation mechanism, we prepared four retinal analogs with a two-carbon bridge linking C_{10} and C_{13} of retinal as part of a cyclohexene ring (10, 11, 21) (see "Experimental Procedures") which permanently fixes the C_{11}=C_{12} bond in the *cis* configuration (Fig. 1*A*). 11-*cis*-Locked isomers were separated by normal phase HPLC (Fig. 1*B*), and their structures were confirmed by mass spectrometry (Fig. 1*C*) and NMR (not shown).

Photoisomerization of Rhodopsin Regenerated with 11-cis-Locked Isomers—All 11-*cis*-locked retinal isomers were stable in solution; however, these isomers could be converted into each other in solution by a short bleach (for example, bleaching of 11-*cis*-locked isomer **3** is shown in Fig. 2, *A* and *B*), with isomer **1** produced in the lowest abundance. To ensure quantitative extraction, particularly in the presence of biological membranes (see below), each isomer was pre-column derivatized with hydroxylamine, and *anti*-oximes were fully chromatographically resolved, while *syn*-oximes were only partially resolved (Fig. 2*B*). As shown in Fig. 3, all four 11-*cis*-locked isomers in solution individually give rise to a mixture of *anti*-oximes after photobleaching. In contrast, when reacted with opsin in native membranes, in the absence of bleaching, 9,11,13-tri-*cis*- (**1**), 11,13-di-*cis*- (**2**), and 9,11-di-*cis*- (**4**) locked retinal analogs spontaneously isomerized to each other (Fig. 3) because of isomerization around the C_{13}–C_{14} bond. This observation is consistent with earlier studies with di-*cis*-retinals that showed that the *cis* C_{13}=C_{14} bond is destabilized upon reaction with opsin (22). 11-*cis*-Locked analog **3** did not isomerize after binding to opsin (Fig. 3). Bleaching of 11,13-di-*cis*- (analog **2**) and 11-*cis*-locked (analog **3**) rhodopsin produced isomerization around the C_9=C_{10} double bond. Quantitative analysis of the 9,11,13-tri-*cis* and 9,11-di-*cis* locked retinal

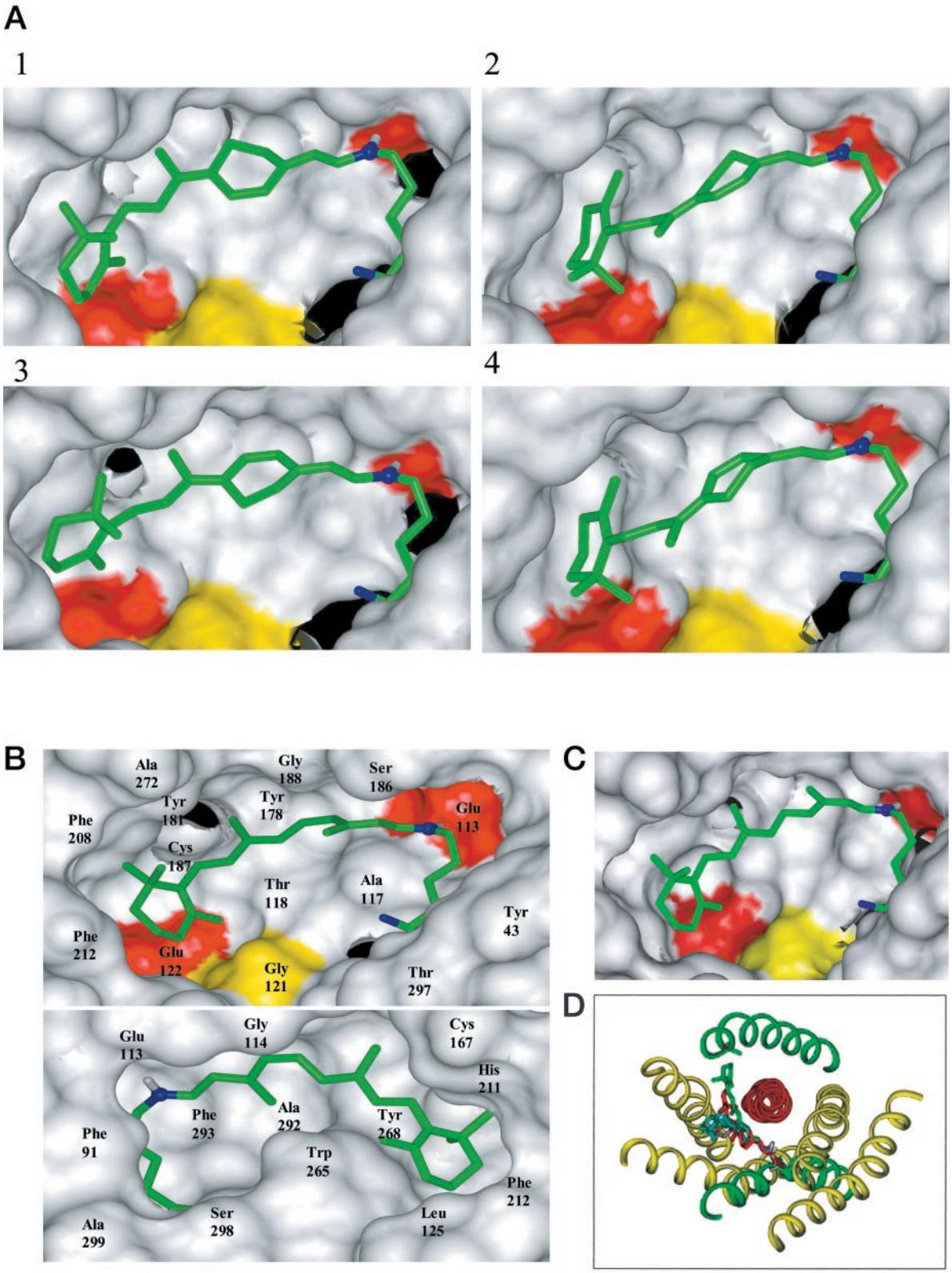

FIG. 4. **The structure of 11-*cis*-retinal and four 11-*cis*-locked isomers in the binding pocket of bovine opsin (5).** *Panel A*, four 11-*cis*-locked isomers in the binding pocket of rhodopsin. Nitrogen atoms of the peptide bond and a Schiff base, with the hydrogen, between Lys^{296} and the retinal are in *blue*. Two acidic residues in the binding site, Glu^{113} and Glu^{122} close to the β-ionone ring, are in *red*. *Panel B*, *top*, residues within 4.5 Å distance from retinal and Lys^{296} (shown in *stick model*). Residues 265, 268–269, and 292–295 were deleted to see the retinal inside the binding pocket. *Bottom*, residues within 4.5 Å distance from retinal and Lys^{296} (shown in *stick model*). Residues 117–118 and 121–122 were deleted to see 11-*cis*-retinal inside the binding pocket. *Panel C*, all-*trans*-retinal in the binding pocket of rhodopsin in an early stage of photoactivation (photorhodopsin and bathorhodopsin) is shown. The structure is in agreement with previous studies using retinal analogs (27). *Yellow*, Gly^{121}; *red*, Glu^{113} close to the Schiff base and Glu^{122} close to the β-ionone ring. *Panel D*, summary structure with all-*trans*-retinal (*green*), 11-*cis*-retinal (*blue*), and analogs **1** (*gray*) and **2** (*red*) in the binding site of rhodopsin. Ala^{169} on helix IV is marked in *green*.

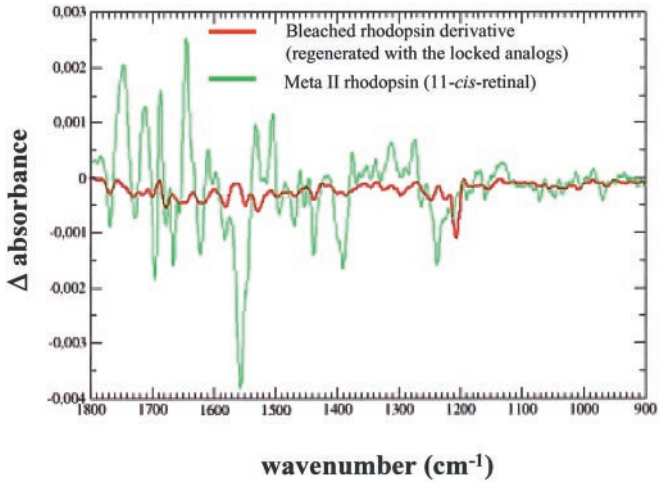

FIG. 5. **FTIR difference spectra of rhodopsin before and after illumination.** *Red*, difference spectrum of rhodopsin regenerated with the mixture of locked retinals; *green*, difference spectrum of the 11-*cis*-retinal regenerated sample (control measurement). Negative bands correspond to vibrations present in rhodopsin, positive bands to vibrations in the photoproduct (for details, see "Results and Discussion").

regenerated rhodopsin was more difficult due to isomerization in the dark; however, all isomers were produced upon photoisomerization. The locked retinal structures differ significantly from each other, and clear specificity is observed with other enzymes utilizing these analogs. Recombinant 11-*cis*-RDH and native 11-*cis*-RDH in retinal pigment epithelium membranes preferred analogs **1** and **3** as substrates ("Experimental Procedures") (13), whereas native and recombinant all-*trans*-RDH (prRDH) was specific toward analogs **2** and **4**. The difference in specificity between these two dehydrogenases results from the recognition of the C_{13}=C_{14}–C_{15} carbon triad configuration in addition to the β-ionone ring (Fig. 3). Thus, rhodopsin's infidelity in discriminating the locked analogs results from the relaxed structural constraints in the active site rather than the structural flexibility of these hydrophobic analogs.

These results surprisingly reveal that rhodopsin regenerated with 11-*cis*-locked retinals readily undergoes photoisomerization (Fig. 3) without or marginal activation of transducin (Table I) (11, 21). These data are consistent with the earlier observation that the spectrum of rhodopsin regenerated with the locked analog **3** changes upon illumination (21). Similar absorption maxima of rhodopsin regenerated with analogs (conformational sensitive opsin shift), ranging from 494 to 510 nm (data not shown), suggest that the interaction of opsin and the chromophore is not considerably changed as a result of the different configuration around the C_9 and C_{13} double bonds found among these analogs. The structural changes in the retinal analogs bound to opsin upon isomerization and how opsin accommodates such changes were investigated utilizing the recently solved high resolution three-dimensional structure of rhodopsin (5).

Locked Analogs in the Active Site of Rhodopsin—All four locked retinal analogs were modeled in the active site of rhodopsin (Fig. 4*A*) ("Experimental Procedures"). These chromophores fit well into the retinylidene binding site. The ϵ-nitrogen of Lys^{296}, in a Schiff base with analogs **1–4**, projects directly toward the Glu^{113} counter-ion, (Fig. 4*A*), which is in agreement with the ~500 nm absorption maximum for rhodopsin regenerated with these analogs. Modeling suggests that fitting analogs **2** and **4** into the binding pocket of opsin requires flipping the β-ionone ring about the C_6–C_7 single bond to give a 6s-*trans* conformation (Fig. 4*A*; see Fig. 1. legend). This repositioning also leads to changes in the location of the cyclohexene ring, compared with isomers **1** and **3**. There is no structural restriction from the protein on conformational changes of the chromophore, as observed experimentally by interconversion of one locked analog into the others. Importantly, the position of the C_{12}–C_{15} region is hardly changed among these four bound retinal analogs. Liu and Mirzadegan (23) proposed a model of the rhodopsin active site from reconstitution studies of rhodopsin with different mono-, di-, and tri-*cis*-retinals and concluded that despite significantly different geometry, for example for 7-*cis*-retinal *versus* 11-*cis*-retinal, the chromophores provide the same "points of anchor," in particular, for the position of the β-ionone ring. With a high resolution structure of rhodopsin and using locked analogs, it appears that these early assertions, despite the rotation of the β-ionone ring, could be valid. FTIR was employed to investigate changes in the hydrogen bonding of rhodopsin, regenerated with the locked retinal analogs and then exposed to light (Fig. 5).

For rhodopsin regenerated with locked analogs, there is a distinct light-induced difference band in the spectrum at 1,206 cm^{-1}. It belongs to the spectral region that reflects light-induced changes in retinal geometry and retinal-protein interaction (fingerprint region). In the same region, the more complex fingerprint of the normal sample is dominated by the 1,238 cm^{-1} band with the same negative polarity. Protonation-dependent bands around 1,700–1,770 are insignificant. The spectral changes in the amide I and II are marginal, indicating lack of major light-induced alterations in the peptide backbone (amide I and II bands at 1,700–1,620 and 1,570–1,500 cm^{-1}, respectively) (Fig. 5). Small spectral changes around 1,768/1,745 cm^{-1} indicate minor changes in hydrogen bonding of Asp^{83} and Glu^{122}. The intensity of the 1,206 cm^{-1} band did not decrease when the sample was treated with 2 mM hydroxylamine or washed extensively with bovine serum albumin. None of the spectral changes was observed in control measurements employing the retinal analogs in alcoholic solution or when added to aqueous bovine serum albumin solution (data not shown). We conclude that, in agreement with the extraction experiments, light-induced changes in the chromophore (different from those seen with C_{11}=C_{12} double bond isomerization) do occur, but the activating structural changes in opsin are absent.

Orientation of the β-Ionone Ring of 11-cis-Retinal in Rhodopsin—The orientation of the β-ionone ring of 11-*cis*-retinal in the crystal structure of bovine rhodopsin (5) (for more detailed analysis, see Ref. 24) is in disagreement with the most recent NMR-derived structure of the chromophore as proposed by Gröbner and colleagues (25). NMR and crystal structure models are very similar for the polyene chain; however, the β-ionone ring is flipped from the 6s-*cis* ($C_5C_6C_7C_8$ torsion angle −72.35 seen in the crystal structure) to the 6s-*trans* configuration observed by NMR. Accommodation of both the 6s-*trans* and the 6s-*cis* conformations in the active site would be possible if the key interaction between opsin and the β-ionone ring of the chromophore (5) does not depend on the specific recognition of three methyl groups of the β-ionone ring (26). Importantly, Ito and colleagues (27, 28) have shown that rhodopsin can be regenerated with 6s-*cis* and 6s-*trans*-11-*cis*-retinal.

Borhan and colleagues (29), employing a photolabeling approach using an 11-*cis*-locked analog similar to **1** but carrying a 3-diazo group on the β-ionone ring, identified Trp^{265} as being in close proximity to the β-ionone ring after photoactivation of the cross-linker (see Ref. 5 and Fig. 4*B*). Based on our studies, it now seems likely that the 3-diazochromophore analog also undergoes photoisomerization to give a mixture of isomers similar to **1–4**. Our modeling studies suggest that only two of

these "locked" analogs (**1** and **3**) would cross-link with Trp^{265} on helix VI, whereas two others (**2** and **4**), resulting from β-ionone flipping, would position the diazo group away from Trp^{265}. The full analysis of the cross-linking studies is complicated by the fact that stoichiometric cross-linking to Trp^{265} was not achieved and the likely possibility that all four chromophore analogs would be present after photolysis (29). Upon illumination of another retinal analog that was photoisomerized to the all-*trans* configuration, a clear movement of the chromophore ring was observed, resulting in cross-linking to Ala^{169} on helix IV (Fig. 4*D*).

The Role of Gly^{121} and C_9 Methyl Group of Retinal—Photoisomerization of rhodopsin reconstituted with locked analogs of retinal but without activation provides additional evidence that changes in the polyene chain configuration and relocation of the C_9 methyl group are insufficient for activation. This observation is also in agreement with an earlier finding that rhodopsin regenerated with an acyclic analog of retinal, lacking a functional β-ionone ring, is not activated upon illumination (30). It has been proposed that Gly^{121} is a contact residue with the C_9 methyl of the chromophore (31); however, the x-ray structure shows that Gly^{121} is more than 4 Å away from the chromophore (Fig. 4, *B* and *C*). However, Gly^{121} could affect packing of residues in the active site in such a way that when Gly^{121} is replaced by other amino acids and 11-*cis*-retinal by analogs containing 9-aliphatic group larger than methyl, this raises the dark activity of rhodopsin depending on the position 121 side chain size and the size of the C_9 substituent of the retinal (31). The C_9 methyl group is, however, essential for complete and efficient transformation of rhodopsin from the early photoproduct to the activated form (32, 33, 34). This observation can be explained by less constrained fitting of 9-demethyl-all-*trans*-retinal into the 11-*cis*-retinylidene binding site compared with all-*trans*-retinal (data not shown).

Activation Mechanism of Rhodopsin—Based on this and previous work, it appears that photoisomerization of the 11-*cis*-chromophore to the all-*trans* configuration causes a twist of the chromophore within the 11-*cis*-retinylidene binding pocket (intermediates known as Photo and Batho) (Fig. 4*C*). Our results suggest that in the next stage, *cis-trans* isomerization causes repositioning of the β-ionone ring which ultimately determines the fate of the receptor activation states. If the photoisomerized chromophore is in an extended conformation, this repositioning of the β-ionone ring is followed by reorganization of transmembrane helix III, and subsequently helix VI (residues 244–276) moves away from H-III (termed Lumi and MI rhodopsins, respectively). This new position of the β-ionone ring initiates, in turn, a sequence of conformational changes (for summary, see Ref. 35) which produces the activated receptor (metarhodopsin II) (Fig. 4*D*). These changes cause deprotonation of the chromophore Schiff base and concurrent protonation of Glu^{113}, and changes on the cytoplasmic surface of rhodopsin (35). If the photoisomerization occurs within the 11-*cis*-retinal binding site, like observed with the locked analogs, despite undergoing isomerization (as shown in this report; see also Ref. 36), there is no (or marginal) activation (Fig. 5 and Table I). In addition, demonstrated plasticity of the binding site, in accommodating different *cis* conformers of retinal (Fig. 4*D*), provides an explanation for the ability to regenerate rhodopsin with drastically different chromophore isomers such as 11-*cis*-retinal, 9-*cis*-retinal, 7-*cis*-retinal, and several di-*cis* derivatives.

Acknowledgments—We are grateful to Preston Van Hooser for sample preparation and support for this project. The computational task was partly done in the ICM computer center, University of Warsaw, Poland.

REFERENCES

1. Palczewski, K., Polans, A. S., Baehr, W., and Ames, J. B. (2000) *Bioessays* **22,** 337–350
2. Sakmar, T. P. (1998) *Prog. Nucleic Acids Res. Mol. Biol.* **59,** 1–34
3. Khorana, H. G. (1999) *J. Biomol. Struct. Design* **1,** 1–16
4. Rao, V. R., and Oprian, D. D. (1996) *Annu. Rev. Biophys. Biomol. Struct.* **25,** 287–314
5. Palczewski, K., Kumasaka, T., Hori, T., Behnke, C. A., Motoshima, H., Fox, B. A., Le Trong, I., Teller, D. C., Okada, T., Stenkamp, R. E., Yamamoto, M., and Miyano, M. (2000) *Science* **289,** 739–745
6. Sakmar, T. P., Franke, R. R., and Khorana, H. G. (1989) *Proc. Natl. Acad. Sci. U. S. A.* **86,** 8309–8313
7. Zhukovsky, E. A., and Oprian, D. D. (1989) *Science* **246,** 928–930
8. Yoshizawa, T., and Wald, G. (1963) *Nature* **197,** 1279–1286
9. Akita, A., Tanis, S. P., Adams, M., Balogh-Nair, V., and Nakanishi, K. (1980) *J. Am. Chem. Soc.* **102,** 6372–6376
10. Zankel, T., Johnson, R. H., Chang, C. W., Sekiya, N., Naoki, H., Yoshihara, K., and Nakanishi, K. (1990) *J. Am. Chem. Soc.* **112,** 5387–5389
11. de Grip, W. J., van Oostrum, J., Bovee-Geurts, P. H., van der Steen, R., van Amsterdam, L. J., Groesbeek, M., and Lugtenburg, J. (1990) *Eur. J. Biochem.* **191,** 211–220
12. van der Steen, R., Groesbeek, M., van Amsterdam, L. J. P., Lugtenburg, J., van Oostrum, J., and de Grip, W. J. (1989) *Recl. Trav. Chim. Pays-Bas* **108,** 20–28
13. Jang, G. F., McBee, J. K., Alekseev, A. M., Haeseleer, F., and Palczewski, K. (2000) *J. Biol. Chem.* **275,** 28128–28138
14. Heck, M., and Hofmann, K. P. (1993) *Biochemistry* **32,** 8220–8227
15. Wessling Resnick, M., and Johnson, G. L. (1987) *J. Biol. Chem.* **262,** 3697–3705
16. Sachs, K., Maretzki, D., Meyer, C. K., and Hofmann, K. P. (2000) *J. Biol. Chem.* **275,** 6189–6194
17. Bartl, F., Ritter, E., and Hofmann, K. P. (2000) *FEBS Lett.* **473,** 259–264
18. Maple, J. R., Huang, M.-J., Stockfisch, T. P., Dinur, U., Waldman, M., Ewig, C. S., and Hagler, A. T. (1994) *J. Comput. Chem.* **15,** 162–171
19. Huang, M.-J., Stockfisch, T. P., and Hagler, A. T. (1994) *J. Am. Chem. Soc.* **116,** 2515–2518
20. Gasteiger, J., and Marsili, M. (1980) *Tetrahedron* **36,** 3219–3222
21. Bhattacharya, S., Ridge, K. D., Knox, B. E., and Khorana, H. G. (1992) *J. Biol. Chem.* **267,** 6763–6769
22. Shichida, Y., Nakamura, K., Yoshizawa, T., Trehan, A., Denny, M., and Liu, R. S. (1988) *Biochemistry* **27,** 6495–6499
23. Liu, R. S. H., and Mirzadegan, T. (1988) *J. Am. Chem. Soc.* **110,** 8617–8620
24. Teller, D. C., Okada, T., Behnke, C. A., Palczewski, K., and Stenkamp, R. E. (2001) *Biochemistry*, in press
25. Gröbner, G., Burnett, I. J., Glaubitz, C., Choi, G., Mason, A. J., and Watts, A. (2000) *Nature* **405,** 810–813
26. Matsumoto, H., and Yoshizawa, T. (1975) *Nature* **258,** 523–526
27. Imamoto, Y., Sakai, M., Katsuta, Y., Wada, A., Ito, M., and Shichida, Y. (1996) *Biochemistry* **35,** 6257–6262
28. Ito, M., Katsuta, Y., Imamoto, Y., Shichida, Y., and Yoshizawa, T. (1992) *Photochem. Photobiol.* **56,** 915–919
29. Borhan, B., Souto, M. L., Imai, H., Shichida, Y., and Nakanishi, K. (2000) *Science* **288,** 2209–2212
30. Jäger, F., Jäger, S., Krutle, O., Friedman, N., Sheves, M., Hofmann, K. P., and Siebert, F. (1994) *Biochemistry* **33,** 7389–7397
31. Han, M., Groesbeek, M., Sakmar, T. P., and Smith, S. O. (1997) *Proc. Natl. Acad. Sci. U. S. A.* **94,** 13442–13447
32. Ganter, U. M., Schmid, E. D., Perez-Sala, D., Rando, R. R., and Siebert, F. (1989) *Biochemistry* **28,** 5954–5962
33. Meyer, C. K., Bohme, M., Ockenfels, A., Gartner, W., Hofmann, K. P., and Ernst, O. P. (2000) *J. Biol. Chem.* **275,** 19713–19718
34. Vogel, R., Fan, G. B., Sheves, M., and Siebert, F. (2000) *Biochemistry* **39,** 8895–8908
35. Okada, T., Ernst, O. P., Palczewski, K., and Hofmann, K. P. (2001) *Trends Biochem. Sci.* **26,** 318–324
36. Sheves, M., Albeck, A., Ottolenghi, M., Bovee-Geurts, P. H. M., De Grip, W. J., Einterz, C. M., Lewis, J. W., Schaechter, L. E., and Kliger, D. S. (1986) *J. Am. Chem. Soc.* **108,** 6440–6444
37. McBee, J. K., Kuksa, V., Alvarez, R., de Lera, A. R., Prezhdo, O., Haeseleer, F., Sokal, I., and Palczewski, K. (2000) *Biochemistry* **39,** 11370–11380
38. Litman, B. J. (1982) *Methods Enzymol.* **81,** 150–153